

## Original Paper

# Controls of accommodation to sediment-supply ratio on sedimentary architecture of continental fluvial successions



Wei Li <sup>a, b</sup>, Da-Li Yue <sup>a, b, \*</sup>, Yu-Shan Du <sup>c</sup>, Jian Li <sup>c</sup>, Chi Zhang <sup>a, b</sup>, Zhi-Qiang Gong <sup>a, b</sup>,  
Xue-Ting Zhang <sup>a, b</sup>, Qing-Lin Shu <sup>c</sup>, Jian Gao <sup>d</sup>

<sup>a</sup> National Key Laboratory of Petroleum Resources and Engineering, China University of Petroleum (Beijing), Beijing, 102249, China

<sup>b</sup> College of Geosciences, China University of Petroleum (Beijing), Beijing, 102249, China

<sup>c</sup> Shengli Oil Field Company, SINOPEC, Dongying, Shandong, 257015, China

<sup>d</sup> PetroChina Research Institute of Petroleum Exploration & Development, Beijing, 100083, China

## ARTICLE INFO

## Article history:

Received 12 July 2022

Received in revised form

5 November 2022

Accepted 15 February 2023

Available online 10 March 2023

Edited by Jie Hao and Teng Zhu

## Keywords:

Channel body

Sedimentary architecture

Stacking pattern

Formative river type

Sequence stratigraphy

A/S

## ABSTRACT

The applicability of sequence stratigraphic models to continental fluvial successions has long been topic for debate. To improve our understanding of how fluvial architectures record responses to changes in the ratio between accommodation rate and sediment-supply rate (A/S), two case studies are analyzed, including a densely drilled subsurface fluvial reservoir imaged with a seismic cube, and an outcropping fluvial succession. The subsurface dataset provides a larger, three-dimensional perspective, whereas the outcrop dataset enables observation at higher resolution. On the basis of both datasets, channel-body density, channel-body stacking patterns and their formative river types are interpreted at different scales, and how these may reflect responses to A/S change (the rate of accommodation creation relative to the rate of sediment supply) are discussed. The results indicate that (i) channel-body stacking patterns undergo four evolutionary stages along with the A/S increase, i.e., multi-story, mixed multi- and two-story, two-story, and isolated patterns; (ii) channel-body density decreases along with the channel-body stacking patterns varying from multi-story to isolated; (iii) formative rivers types are interpreted as evolving from braided planforms to braided-meandering planforms and then to meandering ones, with the increase of A/S.

© 2023 The Authors. Publishing services by Elsevier B.V. on behalf of KeAi Communications Co. Ltd. This is an open access article under the CC BY-NC-ND license (<http://creativecommons.org/licenses/by-nc-nd/4.0/>).

## 1. Introduction

The applicability of sequence stratigraphic models as a correlation tool or a predictor of fluvial architecture for continental fluvial strata is a controversial topic (Shanley and McCabe, 1994; Miall, 2010; Martinus et al., 2014; Colombero et al., 2015). The early sequence stratigraphic models of nonmarine depositional systems emphasized accumulation as primarily determined by the sea level, with a special focus on the highstand phase of a sea-level cycle (Posamentier et al., 1988; Posamentier and Vail, 1988). This concept was then examined and questioned by a series of fluvial sequence stratigraphy studies (e.g., Miall, 1991; Schumm, 1993; Wescott, 1993; Shanley and McCabe, 1994). In these studies, it was argued

that sea-level changes indeed affect the river aggradation and degradation in the distal reaches of fluvial systems close to the shoreline, but may have only limited impact on upstream fluvial systems located far away from the shoreline (Miall, 1991; Shanley and McCabe, 1994). For these upstream rivers, changes in water discharge and sediment flux (sediment supply), resulting from climate changes and tectonism, can override sea-level changes (Schumm, 1993; Wescott, 1993; Holbrook and Schumm, 1999; Miall, 2010; Mueller and Pitlick, 2014; Colombero et al., 2017). Furthermore, some studies argue that the fluvial base level at regional scales, rather than the marine base level (i.e., the sea level), is more broadly applicable to fluvial systems, especially for rivers located in nonmarine basins or far away from the shoreline (Shanley and McCabe, 1994; Holbrook et al., 2006; Martinus et al., 2014). The accommodation generated by regional base-level change is therefore considered an important control of fluvial architecture (e.g., Wright and Marriott, 1993; Shanley and McCabe, 1994; Catuneanu et al., 2009). However, a meta-study of 20 field

\* Corresponding author. State Key Laboratory of Petroleum Resources and Prospecting, China University of Petroleum (Beijing), Beijing, 102249, China.

E-mail addresses: [wei\\_li@cup.edu.cn](mailto:wei_li@cup.edu.cn) (W. Li), [yuedali@cup.edu.cn](mailto:yuedali@cup.edu.cn) (D.-L. Yue).

examples performed by Colombera et al. (2015) suggests that the rate of accommodation generation is not a reliable predictor of aspect of fluvial architecture, such as the channel-body geometry, density, and stacking pattern. Thus, fluvial sequence stratigraphy is still debated, particularly with regards to geological controls and their effects on the sedimentary architecture of fluvial depositional systems (e.g., Shanley and McCabe, 1994; Catuneanu et al., 2009; Colombera et al., 2015).

Nonetheless, rates of accommodation generation and sediment supply are widely considered as key controlling factors (Cross, 2000; Holbrook et al., 2006; Mueller and Pitlick, 2014; Gong et al., 2019; Yan et al., 2020), and their ratio (A/S, see below for the definition) can therefore be considered as a critical control on sedimentary architecture (Cross, 2000; Holbrook et al., 2006; Fanti and Catuneanu, 2010; Miall, 2010; Li et al., 2015). Therefore, geologists, and especially petroleum geologists, have produced a sizeable body of research in three areas: (i) investigating the relationships between A/S and sedimentological and stratigraphic attributes, such as facies diversity and sedimentary architectures in fluvial hydrocarbon reservoirs (Cross, 2000; Ghinassi et al., 2016; Li et al., 2015; Yao et al., 2018; Yue et al., 2018); (ii) using inferred changes in A/S as a correlation tool in continental strata (Zheng et al., 2001; Martinus et al., 2014; Li W. et al., 2020b); and (iii) trying to apply the established relationships in the exploration and characterization of hydrocarbon reservoirs (Cross, 2000; Deng, 2009; Martinus et al., 2014; Melo et al., 2021). The first research topic is the core subject of fluvial sequence stratigraphy, and forms the basis of the other two applied topics. Despite significant advances made in the past thirty years, there is no accepted view on what may be the common relationships between fluvial architecture and A/S change (Cross, 2000; Holbrook et al., 2006; Rook et al., 2010; Martinus et al., 2014; Colombera et al., 2015). In particular, a limited number of publications illustrate the relationship between A/S changes and the transition in river planform between braided and meandering.

Therefore, this work aims to improve our understanding of relationships between fluvial architecture and A/S changes, particularly in terms of responses of the formative river type, channel-body density and stacking patterns. To achieve this objective, a subsurface fluvial reservoir and a fluvial outcrop are studied, and their formative rivers are interpreted to have multiple planform types, including braided, braided-meandering (i.e., termed transition rivers between braiding and meandering, or wandering planforms) and meandering rivers. The subsurface dataset provides a larger, three-dimensional (3D) perspective, whereas outcropping successions allow observations to be made at a higher resolution; the integration of these datasets can contribute to the investigation of fluvial architectures at different scales.

## 2. Concepts and recognition of A/S change

### 2.1. Concepts of accommodation and A/S

Sediment accommodation is originally defined as “the space available for potential sedimentation” by Jervey (1988). In marine basins, the rate of creation of accommodation is a function of both rates of sea-level fluctuation and rates of subsidence, since accommodation is equivalent to the space between the depositional interface and the sea level (Jervey, 1988). However, the marine base level (i.e. the sea level) has no practical meaning in fluvial environments placed far away upstream of the shoreline (Miall, 1991; Holbrook et al., 2006; Martinus et al., 2014). The river “graded” (or equilibrium) profile (Mackin, 1948) therefore is used commonly as the fluvial base-level in studies of fluvial sequence stratigraphy (Cross, 2000; Holbrook et al., 2006; Miall, 2010; Martinus et al.,

2014). The river graded profile is defined as a conceptual, equilibrium surface, which rivers strive to reach through aggradation or incision (Mackin, 1948; Holbrook et al., 2006); this graded profile is determined by the interaction between stream flow and channel characteristics (Howard et al., 1994; Merritts et al., 1994; Tebbens et al., 2000).

Studies on modern rivers indicate that the river graded surface is dynamic and not static, fluctuating to balance out the discharge and sediment flux through erosion and aggradation (Knighton, 1988). The zone between the upper and lower limits of this profile fluctuation is considered the potential accommodation of fluvial depositional systems (Fig. 1) (Cross, 2000; Holbrook et al., 2006; Miall, 2010; Martinus et al., 2014). For a short time scale, e.g., a fifth-order sequence stratigraphic cycle (corresponding typically to a parasequence), the floodplain surface is a common proxy of the upper limit of the river graded profile, whereas the river thalweg acts as proxy of the lower limit (Wright and Marriott, 1993; Blum and Törnqvist, 2000; Holbrook et al., 2006; Martinus et al., 2014) (Fig. 1). This modified definition of accommodation creation has been used widely in studies of fluvial sequence stratigraphy, because it can be estimated relying on observations made in preserved fluvial succession in the rock record (Cross, 2000; Holbrook et al., 2006; Miall, 2010; Martinus et al., 2014).

In studies of sequence stratigraphy, the rate of accommodation creation (A) is commonly considered relative to the rate of sediment supply (S), which is commonly expressed in terms of A/S (also named as A/S ratio and  $\Delta A/\Delta S$ ) (e.g., Cross, 2000; Martinus et al., 2014; Ainsworth et al., 2018; Colombera and Mountney, 2020).

### 2.2. Recognition criteria of A/S changes

Changes in the A/S ratio are expected to produce variations in river geomorphology and sedimentary process, thereby result in significant differences in the stratigraphic and sedimentary architecture of fluvial successions (Knighton, 1988; Schumm, 2005; Miall, 2010; Martinus et al., 2014). Given the objective of further understanding the responses of fluvial architecture to A/S changes, indicators of A/S change that are broadly adoptable and genetically related to the rate of sediment supply and/or accommodation creation are summarized on the basis of previous studies, whereas others related to fluvial architecture were ignored in this work; these are as follows:

- (i) Relative proportion of fluvial sandstone in a zone corresponding to a fifth- or sixth-order cycle. The thickness of the preserved zone is a critical proxy of accommodation creation in a fluvial depositional system (Holbrook et al., 2006). Changes of the fluvial sandstone proportion indicate variations in sediment flux and discharge, and thereby indicate changes of sediment supply rate (Knighton, 1988). Therefore, the decrease of fluvial sandstone proportion commonly indicates a rising A/S in fluvial strata (Cross, 2000; Schumm, 2005; Holbrook et al., 2006).
- (ii) Relative proportion of fine-grained deposits preserved in fluvial elements of different hierarchies, especially for the individual and compound channel belt. The proportion of fine-grained deposits indicates the variation in accommodation generation as well as in sediment supply rates (Schumm, 2005). An increasing A/S condition commonly leads to a higher proportion of fine-grained deposits in the individual and compound channel belts (Schumm, 2005; Holbrook et al., 2006; Martinus et al., 2014).
- (iii) The grain size of channel sandbodies across each zone. Changes in channel-deposit grain size are partly related to variations in accommodation generation and in sediment

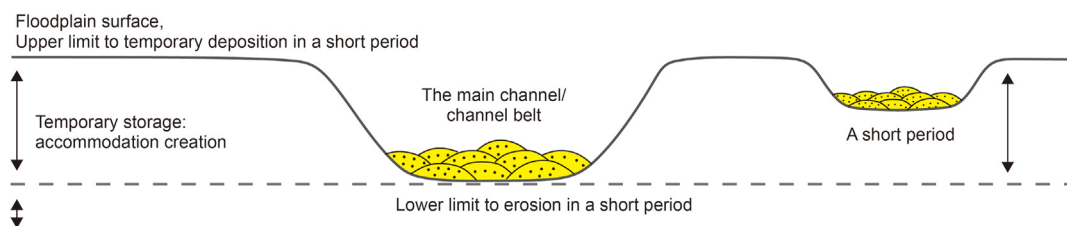


**Fig. 1.** Definition of accommodation creation in fluvial depositional systems, for a short period corresponding to a fifth-order or a sixth-order cycle (modified after Blum and Törnqvist, 2000). A fifth-order cycle correspond generally to a parasequence (Zheng et al., 2001; Colombera and Mountney, 2020).

supply rates (Knighton, 1988; Schumm, 2005). A larger grain size commonly indicates lower preservation of sediments carried by the stream flow, which suggests a low ratio of A/S. Riverbed gradient is primarily related to sediment grain size and channel depth, and a larger grain size commonly indicates a higher gradient (Trampush et al., 2014). A larger riverbed gradient is corresponding to a higher channel incision capacity and thus leads to a lower of river grade, i.e., a lower fluvial base-level. Therefore, a large grain size of deposits may indicate a low A/S ratio.

- (iv) Degree of palaeosol maturity in profiles. Preserved palaeosols with low to modest maturity degrees can act as indicator of relatively rapid sedimentation (Wright and Marriott, 1993; Knighton, 1988). Increasing palaeosol maturity is a potential proxy of decreasing A/S condition in fluvial strata (Wright and Marriott, 1993; Martinus et al., 2014).

Care must be taken because these A/S change indicators are also partly controlled by the climate, upstream factors of source area, differential subsidence, and downstream factors of sea/lake level (Cross, 2000; Schumm, 2005; Holbrook et al., 2006). It is therefore important to apply them comprehensively rather than in isolation.

### 3. Dataset and methodology

Two case studies of fluvial successions are used to investigate the responses of fluvial architecture to A/S changes, to integrate a high resolution outcrop dataset with the larger 3D perspective offered by the subsurface dataset. Both successions are interpreted to be fluvial in origin, and their formative rivers are interpreted to have had multiple planform types, including braided, meandering and braided-meandering transition rivers (Li et al., 2015, 2019a, 2019b, 2022; Zheng et al., 2000).

#### 3.1. Case study 1: A fluvial outcropping succession

The first case is a fluvial outcropping succession, located 10 km northwest of Datong City, in northern China, at 40°7'29"N, 113°9'32"E. This outcrop consists of 8 sections (sections A-H), with a total height of 140 m, and a total lateral extent of 1300 m. Sections A-C are along a railway cutting, and sections D-H are along a highway cutting (Fig. 2). This outcrop exposes parts of the Yungang Formation of middle Jurassic (Li et al., 2015), when the craton plate subsided slowly and the regional tectonic movements are considered to be mild (Wang, 2001). These exposed Jurassic Yungang Formation were interpreted to be fluvial in origin, and produced by rivers with braided, meandering, and braided-meandering transition planforms (Li et al., 2015; Li et al., 2022). Relationships between the orientation of outcrop sections and the depositional strike of channel belts are shown in Fig. 2d. Fluvial deposits shown in this work are located between 30 km and 60 km far away from the southeast of the mountains (Wang, 2001).

The outcrop dataset used in this work includes (i) outcrop photomosaics, (ii) impregnated thin sections, (iii) grain-size analyses (using a laser particle analyzer), (iv) gamma-ray logs measured with a gamma spectrometer (LAUREL RS-230), and (iv) 3D laser-scan data (FARO Focus3D X330). Grain-size measurements were conducted on 150 rock samples: 57 samples from the outcrop sections A-C, 52 from the outcrop sections D-G, and 41 from the outcrop section H. There are 60 impregnated thin sections in total, 25 from sections A-C, 12 from sections D-F, 8 from section G, and 15 from section H. Relationships between the orientation of outcropping successions and the depositional strike of channel belts are shown in Fig. 3d (see Li et al., 2020a for the measuring method). In this outcrop, the compaction ratio (ratio of original to compacted thickness) of fluvial sandbodies is approximately 1.28 (Li et al., 2020a).

The study routine for the outcrop dataset consisted of two parts: recognition of A/S change, and description of the outcropping successions. For the A/S change recognition, all the four indicators mentioned in Section 2.2 were observed and/or measured relying on the outcrop dataset, and the A/S changes were then recognized based on the four indicators combined. Outcrop sedimentary architectures of different hierarchies were depicted, with focus on: (i) density and stacking relationships of individual channel bodies, (ii) lateral and vertical relationships of smaller channel fills within channel bodies, and (iii) densities and relationships of channel erosion surfaces in channel bodies. In this article, the term 'channel body' is applied to describe the preserved record of an individual channel.

#### 3.2. Case study 2: A subsurface fluvial reservoir

The second case study is a fluvial reservoir of the Chengdao Oilfield (Li et al., 2019a), in the Bohai Bay Basin in China (Fig. 3). The Chengdao Oilfield is located in southeastern Chengbei Salient (Fig. 3b), which lies along the northeastern edge of the Chengning Uplift (Fig. 3a). The Chengning Uplift is a positive structure unit, located in middle of the Bohai Bay Basin (Fig. 3a). The Neogene sequence in the Chengdao Oilfield is an oil-bearing succession, in which the Upper Guantao Formation is the interest interval. The Upper Neogene Guantao Formation (24.6–12.0 Ma) are during the stage of depression period, and terrain of the study area were with a relatively flat terrain in that period (Li et al., 2019a; Yue et al., 2018). The burial depths of this interest interval vary from 1000 m to 1600 m.

The Chengdao Oilfield was brought into production at 1995, and it has accumulated abundant geological, geophysical and production data. The used dataset includes 569 wells and a 3D seismic cube in this study, covering approximately 80 km. The spacing between wells varies between 150 m and 500 m, and their mean value is approximately 250 m for the middle block and less than 350 m for the whole study area. All the wells provide abundant data from wireline logs and petrophysical interpretation, including

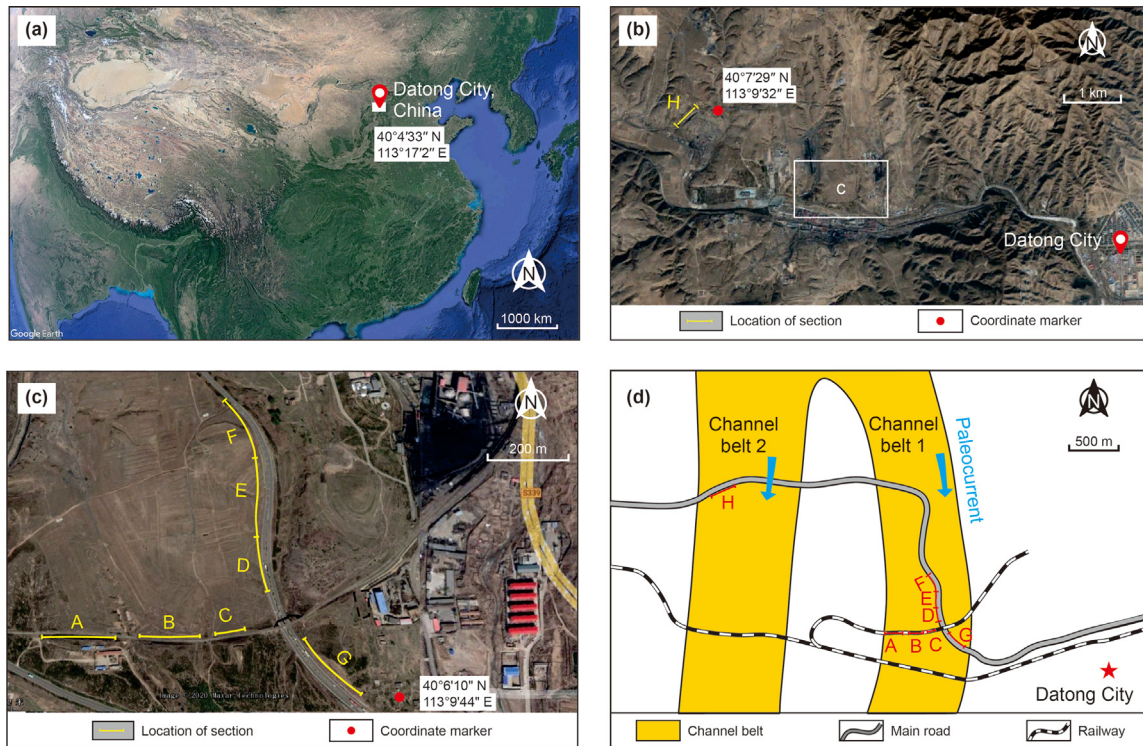


**Fig. 2.** (a–c) Satellite images showing locations of the study outcrop. (a) Location of Datong City. (b) Location of the outcrop section H, in which the white box indicates the location of the part (c). (c) Location of the outcrop sections A–G. (d) Relationships between the orientation of outcrop sections and the depositional strike of channel belts (modified after Yu et al., 2002).

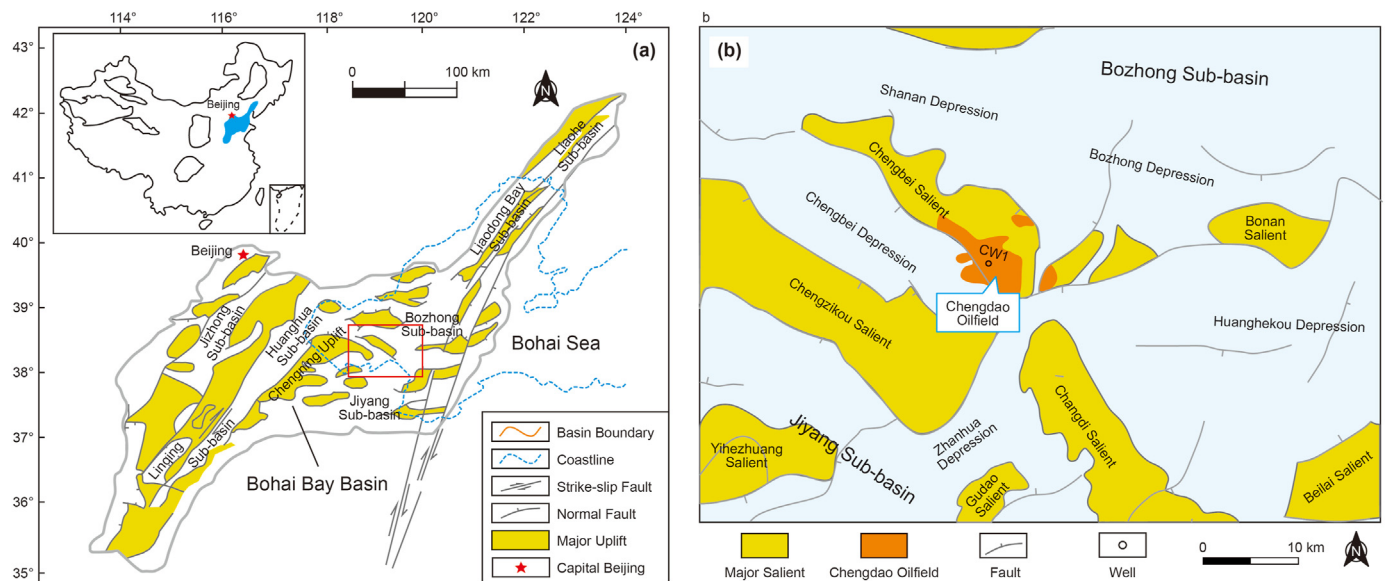


**Fig. 3.** (a) Location and tectonic divisions of the Bohai Bay Basin. The red box is corresponding to the location of part (b). (b) Regional structural features of the central Bohai Bay Basin, and the location of the Chengdao Oilfield (Modified after Li et al., 2019a).

gamma-ray (GR), spontaneous potential (SP), sonic (DT), deep laterolog (LLD), and shallow laterolog (LLS); half of the wells also have density (DEN) logs. Nine of them were cored in the Upper Guantao Formation, which is interpreted to be fluvial in origin (Zheng et al., 2000; Yue et al., 2018; Li et al., 2019a, 2019b). The utilized seismic data were processed to 0-phase, with a dominant frequency of 40 Hz and an effective bandwidth of 18–60 Hz. The vertical sample

interval is 2 ms, and spacings of the inline and common-depth point are both 25 m. The average velocities of sandstone and mudstone are 2650 m/s and 2450 m/s, respectively. Generally, this subsurface case study benefits from a dense array of wells and a high-resolution seismic cube.

The methodology used in the subsurface data also consists of two main parts: recognition of A/S change, and interpretation of

fluvial sandbodies (Fig. 4). Given the limitations of well logs and cores, applicable indicators of A/S change are as follows: (i) relative proportion of fluvial sandbodies in the related reservoir zone (corresponding to a fifth-order cycle), which can be estimated by the ratio of sand thickness to the related zone thickness or by the GR value of each zone, using the dataset of 569 wells; (ii) relative proportion of fine-grained (muddy and silty) deposits preserved in the channel belts, which is estimated relying on the core observations; (iii) the medium grain size of channel sandbodies, which is based on the core grain-size analyses. These three indicators can be applied throughout, whereas recognition of palaeosol maturity can only be made on core observations.

Three methods for sandbody identification were employed in this work, including (i) analyses of frequency-decomposed seismic attributes, (ii) seismic attribute optimization by reducing interferences of neighboring zones, and (iii) frequency-decomposed genetic inversion (Part II in Fig. 4). The first method was proposed by Li et al. (2019a), in which frequency-decomposed seismic attributes are fused with machine learning using a supervised algorithm. This method can readjust the tuning thickness and improve the resolution of seismic interpretation. The second method, which was proposed by Li et al. (2020 and 2021), allows interferences of neighboring zones to be reduced significantly. The third method, proposed by Li et al. (2019b), enables combination of the spectral decomposition and genetic inversion for improving the seismic inversion resolution. Standardized SP logs of 569 wells were the supervised dataset in this inversion work, and the result therefore represents the distribution of SP value and lithology. All these three methods were applied to sandbody recognition in the Chengdao Oilfield, and produced satisfactory results (Li et al., 2019a, 2019b, 2020b, 2021). Sedimentary architecture and formative river types of the fluvial strata were then discussed, based on the predicted fluvial sandbodies.

## 4. Results

### 4.1. Results of the outcropping fluvial successions

#### 4.1.1. A/S changes

The outcropping successions are divided into 11 reservoir zones (Fig. 5), and each of them is corresponding to a fifth-order cycle (parasequence). Each of these zones consists of 2–4 sixth-order cycles (bedsets), as shown in Fig. 6.

Indicators of A/S changes are calculated relying on the outcrop dataset from zones 1 to 11, including: (i) the mean GR value (ii) the relative proportion of sandbodies, (iii) the relative proportion of fine-grained deposits in channel body, and (iv) the medium grain size of sandstone (Fig. 5). Each sixth-order cycle produced a calculated result (the dots in Fig. 5). All these four indicators show a similar trend, with only limited differences. These indicators were normalized and then synthesized to an integrated trendline, aiming at considering all these quantitative parameters. In addition, palaeosols are observed in zones 8, 7 and 3, and the degree of palaeosol maturation in zones 7 and 8 is higher than that in zone 3, suggesting that the A/S ratio in zones 7 and 8 is smaller than that in zone 3. To sum up, these indicators indicate that the A/S ratio increases from zones 11 to 9 and from zones 9 to 1, respectively, with a short-term decrease from zones 9 to 8, bottom-up process (Fig. 5).

#### 4.1.2. Depiction and interpretation of fluvial architecture

The outcropping successions, i.e., zones 1–11, show significant variations on fluvial architectures and their formative river types (Figs. 6 and 7). Successions of zones 9–11 are depicted in outcrop section G (Fig. 6). Successions of zones 6–8 show similar sedimentary features, and the reservoir zone 7 is described in Fig. 7h and g, as a representative example. Fluvial architectures shown in zones 1–3 are similar. Successions of zone 2 are described in Fig. 7a

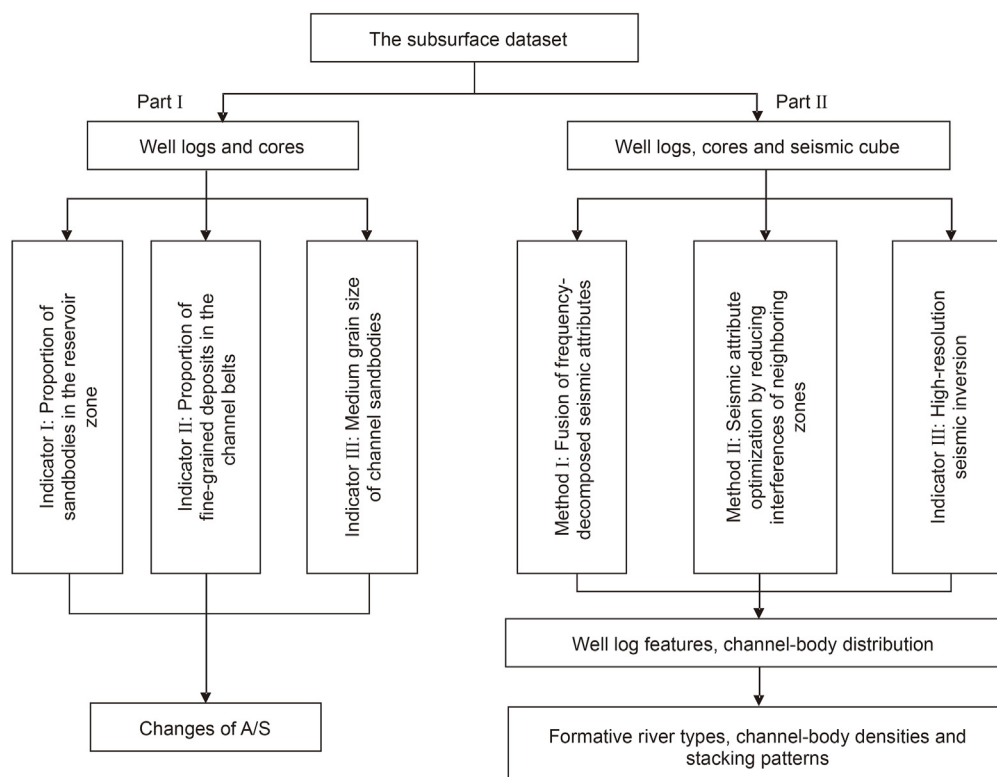
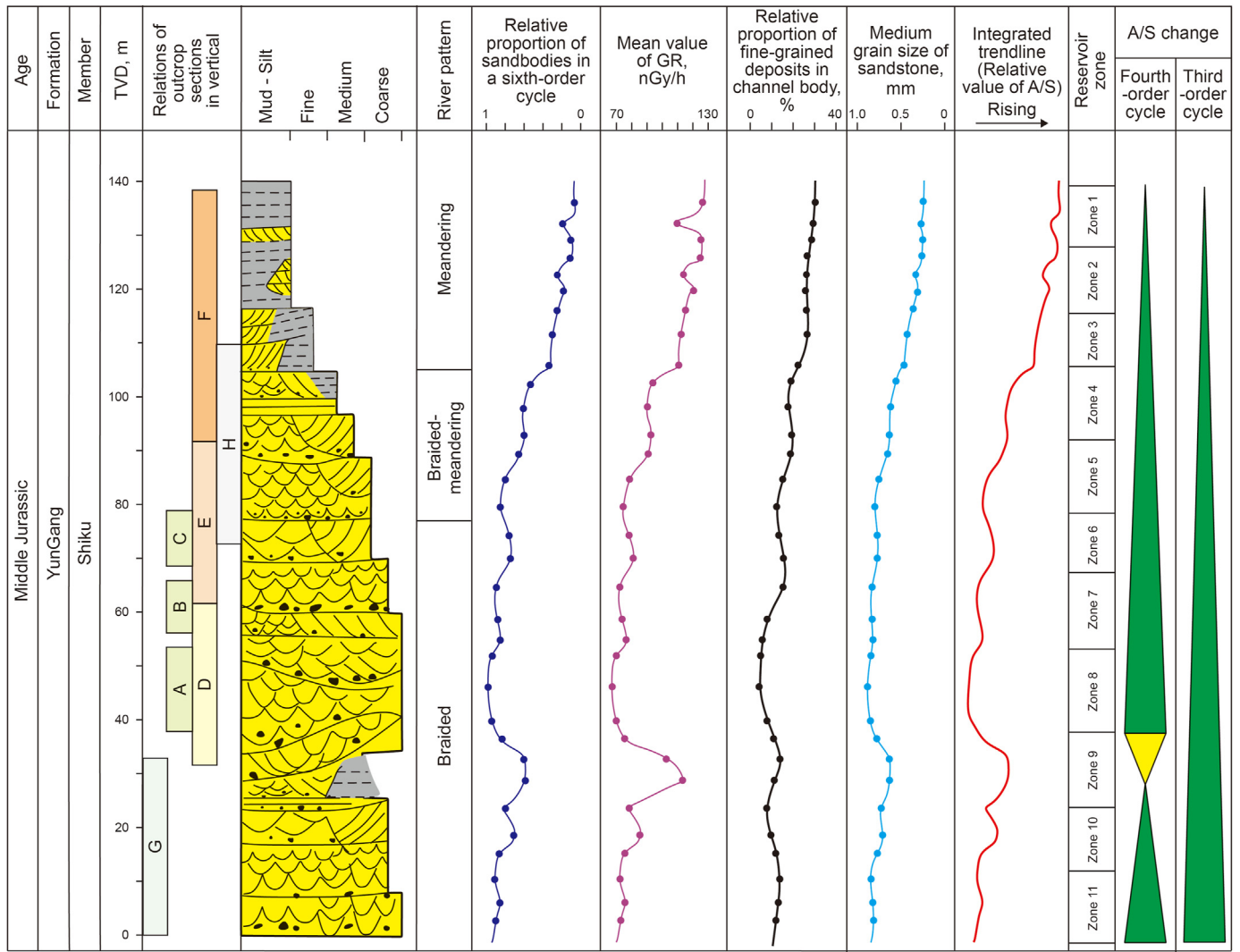


Fig. 4. Workflow diagram outlining the methodology of A/S change recognition and fluvial architecture interpretation.



TVD: True vertical depth

GR: Gamma rays

**Fig. 5.** Analysis diagram of A/S change for the outcrop dataset, including the lithofacies profile, mean GR value, relative proportion of sandstone, relative proportion of fine-grained deposit in channel bodies, medium grain size of sandstone, and their integrated trendline. A dot represents a single calculated value. The third-order cycle is a fluvial sequence, and the fourth-order cycle represents a parasequence set. The mean value of GR logs was modified after (Li et al., 2022).

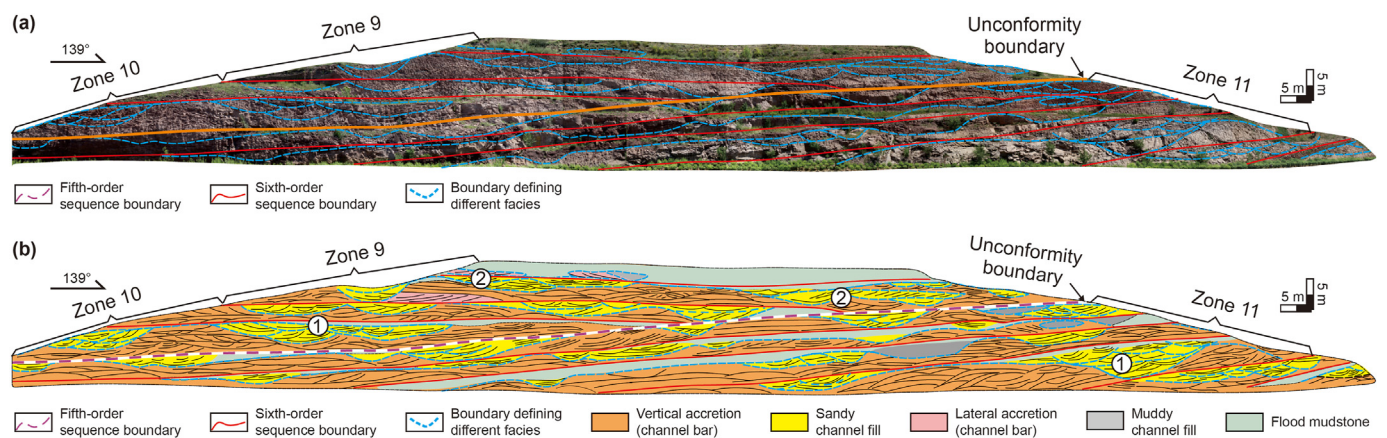


**Fig. 6.** (a) Photomosaic of outcrop section G, showing the fifth- and sixth-order sequence boundaries, and boundaries defining different faices. (b) Depiction and interpretation of fluvial architecture. The exposed successions are zones 9–11, top to bottom.

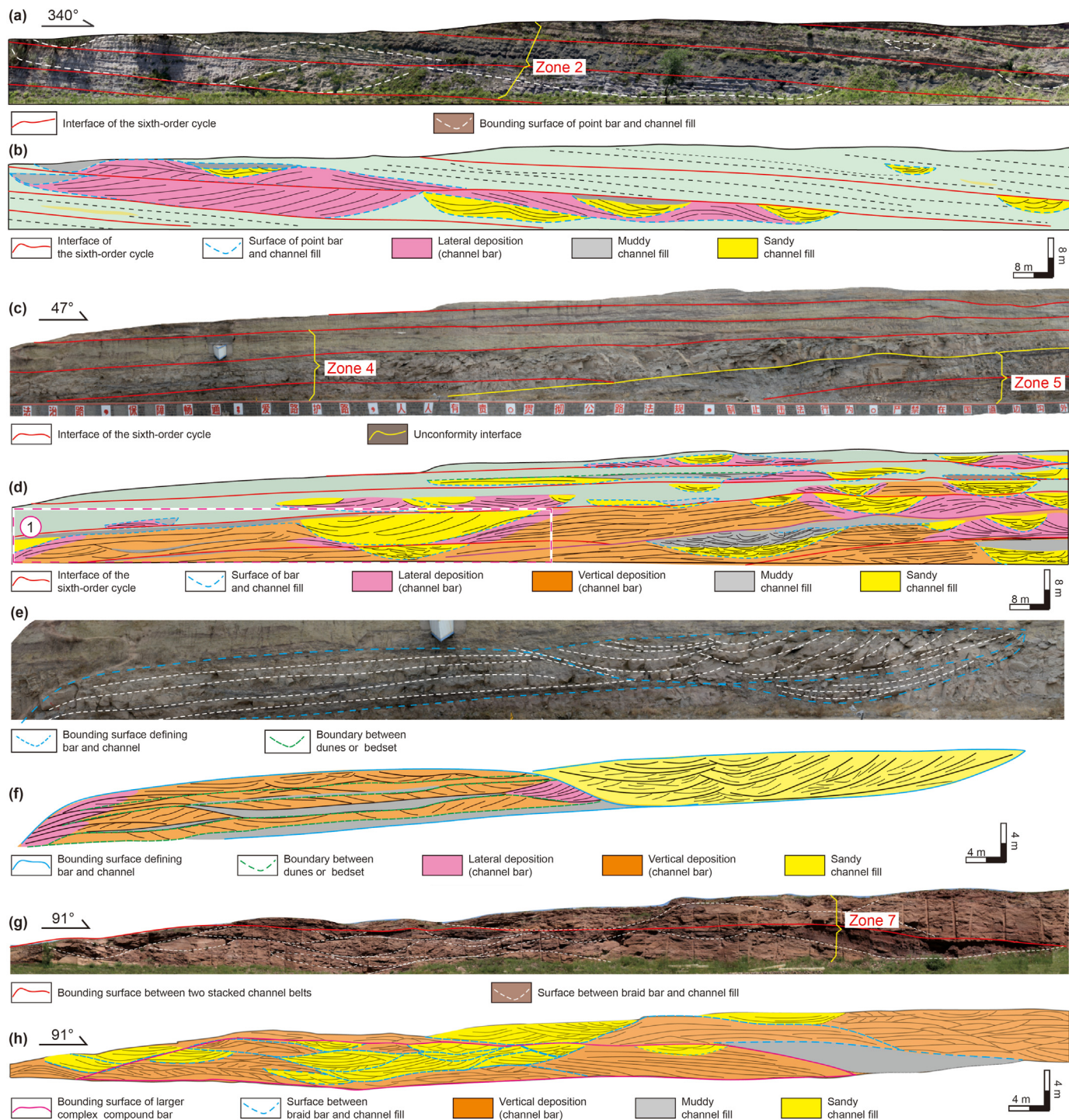


**Fig. 7.** Photomosaics and their depictions of fluvial architecture. (a–b) Part of outcrop section F, corresponding to zone 2, considered typical meandering depositional systems. (c–d) Part of outcrop section H, corresponding to zones 4 and 5, considered braided-meandering river depositional systems. (e–f) Zoom of the rectangular area in part (d). (g–h) Outcrop section B, corresponding to zone 7. The photomosaic shown in part (g) is modified after Li et al., 2022.

and b, whereas successions of zones 4 and 5 are depicted in Fig. 7c and f. Vertical relationships of the outcrop sections A–G are shown in Fig. 5.

Well-exposed successions are divided into three zones (zones 11–9) in section G, with an unconformity acting as the boundary between zones 10 and 11 (Fig. 6). Generally, fluvial sandbodies are the dominant feature until the most recent deposits (sixth-order cycle) of zone 9, in which muddy floodplain sediments become

dominant instead. In zones 10 and 11, channel bodies are stacked in a high density, showing a multi-story stacking pattern. In channel fills, erosion surfaces occur frequently in zones 10 and 11 (channel fill ① for example in Fig. 6), whereas the frequency of erosion surfaces decreases to a moderate degree in zone 9 (channel fill ② for example in Fig. 6). Vertical aggradation is dominant in fluvial bars of zones 9–11, whereas limited lateral accretion is observed in zone 9. Erosion surfaces and large trough cross-stratifications are

very common in these fluvial (compound) bars, suggesting the instability of channels during their evolution. According to sedimentary features shown in Fig. 6, the successions exposed in section G are considered as the preserved expression of braided depositional systems, which is in line with previous understanding (Ren et al., 2018; Li et al., 2020a).

The sedimentary architecture shown in section B (as a representative example of zones 6–8) is broadly similar to that in zone 11, and the successions are also considered as associated with braided rivers. In particular, the frequency of erosion surfaces is very high in channel fills and braided bars; smaller bars and their related channel fills may assemble into larger, complex compound bar (Fig. 7g). This phenomenon results from rapidly migrating unstable channels (Miall, 2010). Also, the geometries of individual channel cross-sections are symmetrical or approximately symmetric, suggesting that the secondary flow is weak during their sedimentary process.

Four significant differences are observed in the successions of zones 4–5 (Fig. 7d–f), compared to the fluvial architecture of zone 7 (Fig. 7g and h). Firstly, the degree of lateral accretion increases within compound bars, although vertical aggradation is still dominant. Mid-channel bars with vertical aggradation and point

bars with lateral accretion are observed in the same channel belt (Fig. 7d); in the mid-channel bar, a few lateral accretion packages lie along their flanks (Fig. 7e and f). Secondly, the frequency of erosion surfaces within the channel body decreases sharply. Thirdly, cross-stratified sets are sometime separated by thin, horizontal, fine-grained layers in the mid-channel compound bar (Fig. 7e and f). At last, some channel fills show obviously asymmetrical cross-sections, suggesting that the secondary flow is relatively strong. Therefore, successions of zones 5 and 4 are interpreted to be braided-meandering river depositional systems, comparable to so-called ‘wandering’ planforms.

In zones 1–3, floodplain deposits are dominant, with few isolated channel sandbodies encased in the mudstone. The channel belt consists of channel fills and point bars, and so these successions are considered typical of meandering depositional systems (Fig. 7a and b).

#### 4.2. Interpretation of the subsurface fluvial reservoirs

##### 4.2.1. A/S changes

The study interval is part of the Neogene Guantao Formation, and is named as sand groups of Ng4 and Ng5 (Fig. 8). This study

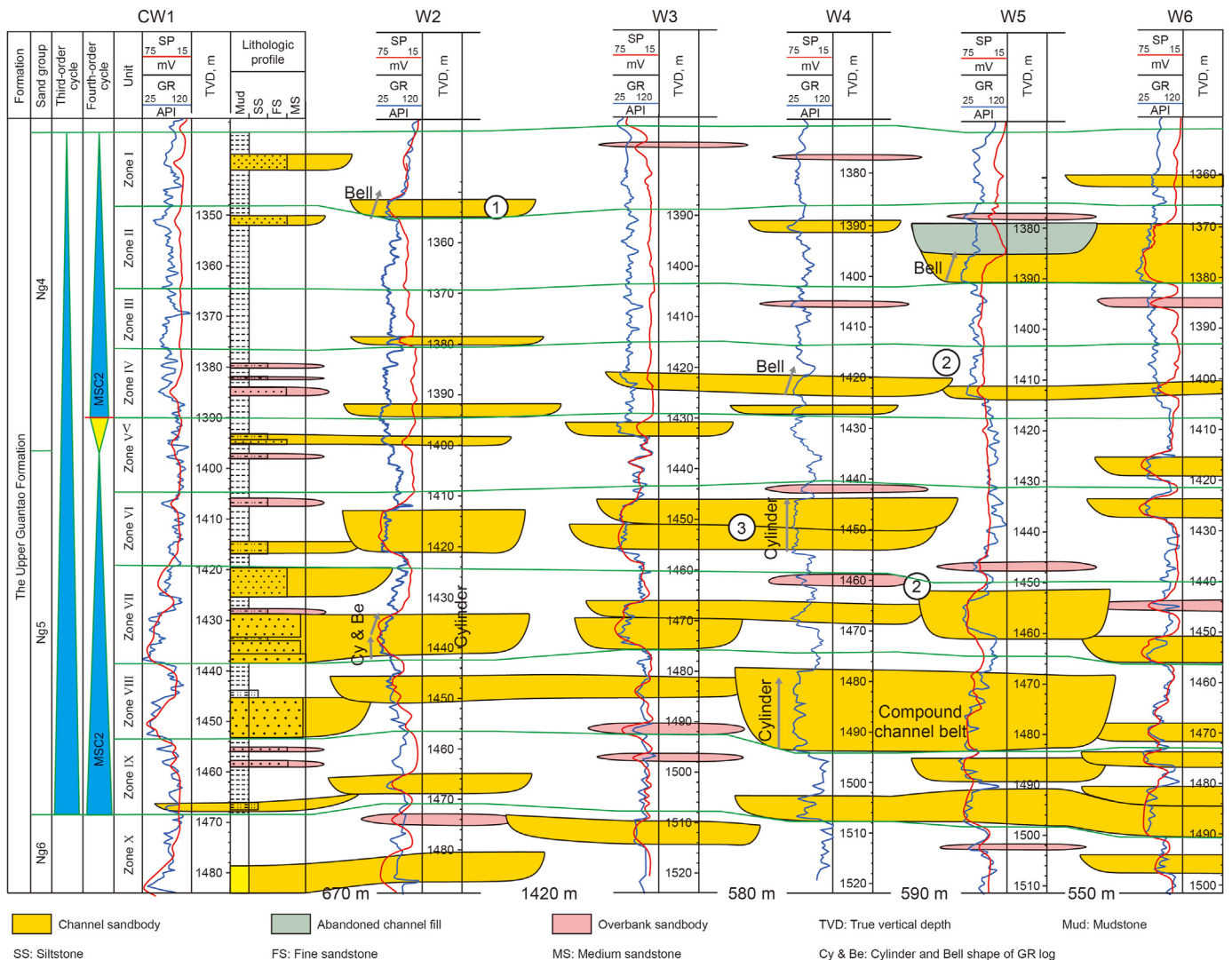


Fig. 8. Well-correlation panel showing the reservoir zones and distribution of fluvial sandbodies in the Upper Guantao Formation, Neogene. Well ‘CW1’ was cored. The section location is shown below. Areas ① - ④ indicate four kinds of channel-body stacking patterns, which were interpreted using the well data and seismic interpretation, see below.



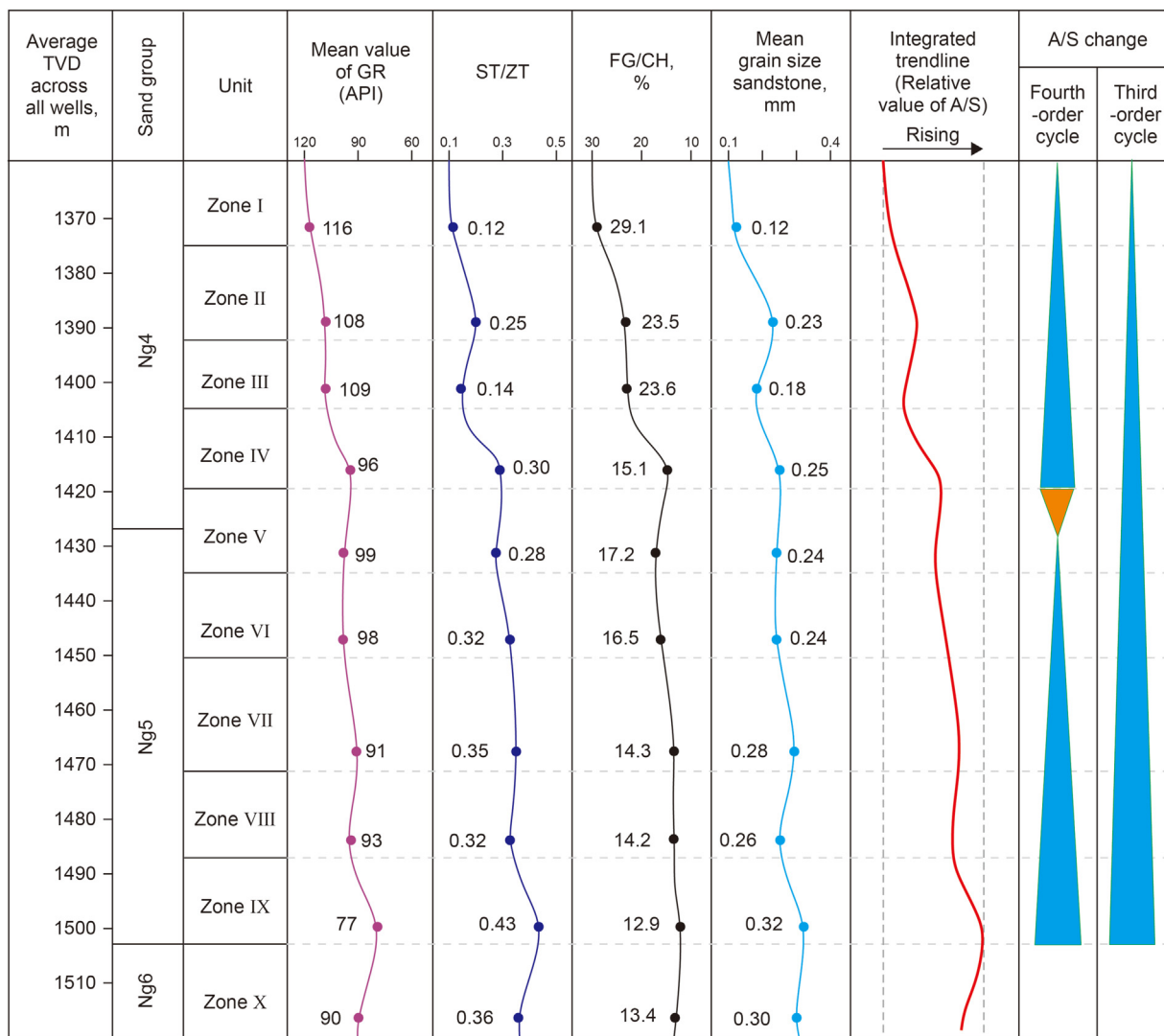
interval is commonly divided into 9 reservoir zones (zones I to IX) on the basis of a series of geological studies (Yue. et al., 2018; Li et al., 2019a), and each of them is approximately corresponding to a fifth-order sequence cycle, with a thickness ranging from 10 m to 20 m (Fig. 8).

Indicators of the A/S change were observed and analyzed relying on cores and well logs, including the (i) ratio of sand thickness relative to the reservoir zone thickness, (ii) mean values of GR across each zone, (iii) relative proportion of fine-grained (muddy and silty) deposits preserved in the channel belt, and (iv) the medium grain size of channel sandbodies. These four parameters show a similar trend, although minor discrepancies are shown between their amplitudes. To consider all these quantitative indicators, they were normalized and then synthesized into an integrated trendline (Fig. 9). All these results indicate that the A/S ratio increases from zone IX to zone I in general, with a minor decrease in from zone V to zone IV (Fig. 9).

#### 4.2.2. Formative river types

The GR-log shape is a common sedimentary facies indicator in

fluvial depositional systems (Rider, 1990). The bell-shaped GR log is a well-known indicator of fluvial fining-upward cycle (Fig. 10a), and the cylinder-shaped GR log represents a fluvial sandbody with a rather constant grain size (Fig. 10b). Meandering channel belts are commonly characterized by a bell-shaped GR log response, including both point bars and channel fills. In braided belts, channel fills still present a bell-shaped response, whereas braid bars are commonly featured with a cylinder-shaped GR log response. The GR log response of bell-cylinder shape (Fig. 10c) is also common in braided belts, resulting from the relationship of channel fills lying on a braided bar. Shapes of the GR log response were observed and counted throughout 569 wells (Fig. 10d). The statistics indicate that the proportion of bell-shaped response decrease from the reservoir zone I to zone IX in general, whereas the total proportion of cylinder and bell-cylinder shaped responses increases (Fig. 10d). Specifically, the bell-shaped response of GR logs takes up a large portion (85–90%) in zones I to III, but less than a quarter in zone IX. According to relative proportions of different GR-log responses, successions in zones I to V and in zones VIII to IX are considered as dominantly the products of meandering and braided river systems,



ST/ZT: Ratio of sand thickness relative to the zone thickness

FG/CH: Proportion of fine-grained deposit in the channel sandbodies

Fig. 9. Analysis of indicators of A/S changes for the subsurface dataset, including the mean GR value of each reservoir zone, the ratio of sand thickness to the related zone thickness, relative proportion of fine-grained (muddy and silty) deposits in fluvial belts, and mean grain size of sandstone in each zone. The dots represent the calculated values of each zone.

respectively, whereas deposits in zones VI to VII are interpreted to be a record of braided-meandering (wandering) river depositional systems.

#### 4.2.3. Distribution of fluvial sandbodies

The fluvial sandbodies in zones I to V can be mapped using both the fusion of frequency-decomposed seismic attributes (Li et al., 2019a) and the frequency-decomposed genetic inversion (Li et al., 2019b). The map of zone II, for example, is produced from the seismic inversion (Fig. 11a), which allows imaging the distribution of channel belts clearly. Afterward, fluvial sandbodies and facies were further interpreted (Fig. 11b), integrating the inversion result and well-log interpretation. This study workflow was detailed by Li et al., 2019b.

The seismic attribute optimization by reducing interferences of neighboring zones produced a better result on sandbody prediction of zones VI to IX, where channel belts are commonly stacked approximately vertically and close to each other, as shown in Fig. 8. The optimized attributes in zone VI, for example, show the distribution of fluvial sandbodies clearly (Fig. 11c and c). Given that the sand thickness interpreted by well logs acts as the supervised training dataset, the optimized (or fused) attribute represents predicted sand thickness (Fig. 11c). This prediction workflow was proposed and detailed by Li et al. (2020b and 2021). At last, distributions of fluvial sandbodies were interpreted and mapped from zones I to IX (Fig. 12).

#### 4.2.4. Channel-body stacking relationship

Channel-body stacking relations in fluvial depositional systems are classified according to three common patterns, on the basis of

the Datong fluvial outcrop (Figs. 6 and 7) and previous studies; these patterns include (i) isolated stacking, (ii) two-story stacking, and (iii) multi-story stacking (Table 1), in order of increasing channel-body density.

The first pattern represents isolated channel bodies encased in floodplain deposits, which can be identified in well-correlation panels and in the seismic inversion cube, such as the geological model and inversion result of the pattern I in Table 1. The two-story stacking pattern is divided into two sub-patterns, depending on whether the channel bodies are dominantly stacked vertically or laterally (pattern II in Table 1). The contact between the channel bodies is smaller in the former, and larger in the latter sub-pattern. For a well spacing of 250 m, one or no well is drilled through the channel-body stacking area in pattern II<sub>1</sub>, whereas the stacking area may be drilled by two even more wells in pattern II<sub>2</sub> (Table 1). More importantly, these two stacking patterns could be recognized in the seismic inversion profile, in which inversion values indicative of sandstone presence show the geometry of stacked channel bodies (inversion profiles in Table 1). In terms of the multi-story stacking pattern, the typical feature is that multiple potential stacking interfaces between channel bodies can be identified on adjacent wells, in a compound channel belt (geological model of pattern III in Table 1). Due to limitations of seismic resolution, although dense stacking interfaces compound channel belt cannot be imaged exactly, the stacking pattern III could be interpreted by integrating the inversion result and the dense well data (Table 1).

At last, the channel-body stacking patterns were interpreted throughout zones I to IX by integrating the wireline logs of dense wells and the results of frequency-decomposed genetic inversion, as shown in Figs. 8 and 13. All types of channel-body stacking

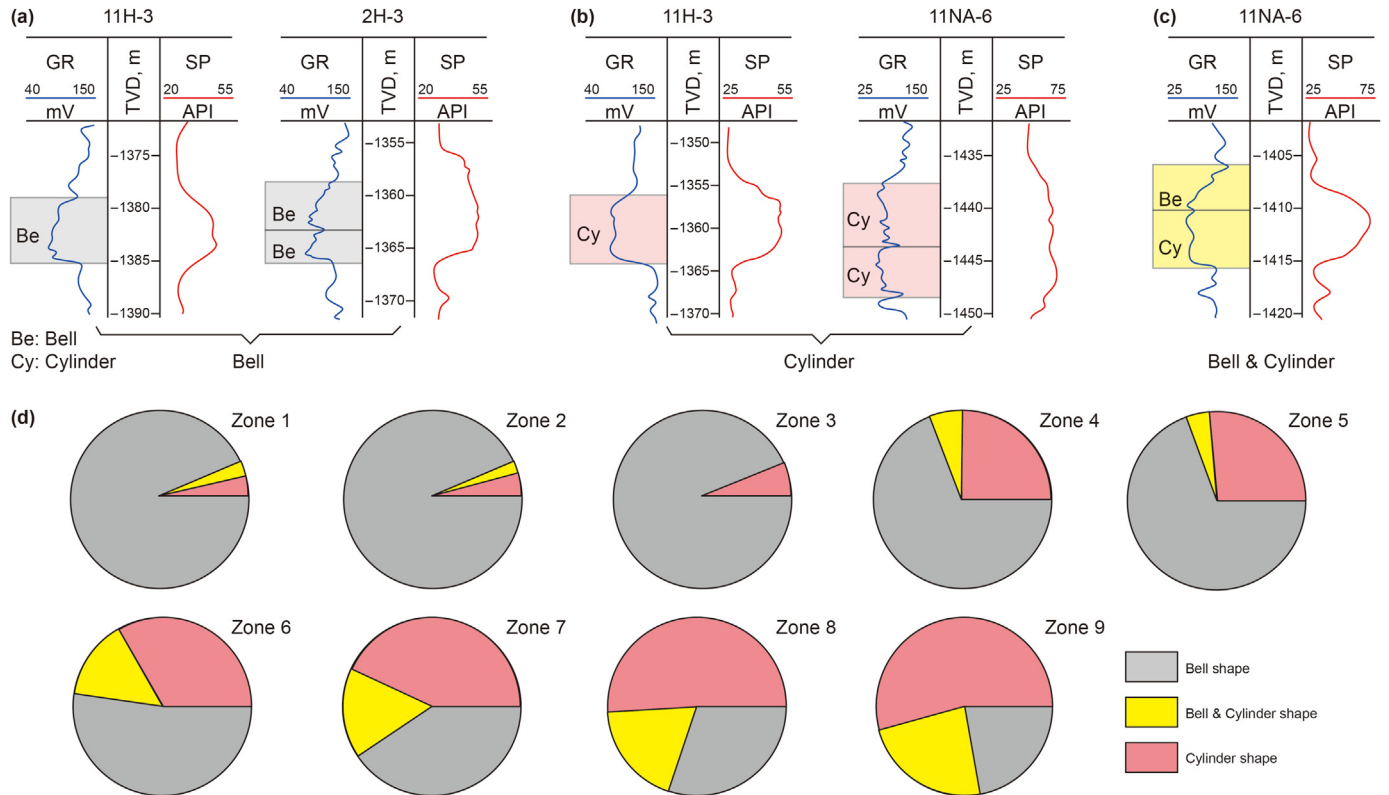


Fig. 10. (a) Bell-shaped GR log responses, showing typical fluvial fining-upward cycles. (b) Cylinder-shaped GR log responses, showing a sandstone with a similar grain size. (c) Bell-cylinder shaped response of GR log. (d) Statistics of GR-log shapes of channel sandbody across zones I to IX, using the 569 wells.

patterns are observed in the study interval, with areas ① - ④ (Figs. 8 and 13) exhibit channel-body stacking patterns I, II<sub>1</sub>, II<sub>2</sub> and III, respectively. The channel-body distribution, in both plan-view (Fig. 12) and cross-section (Figs. 8 and 13), indicates that: (i) isolated channel bodies encased in floodplain deposits (channel-body stacking pattern I) are dominant in zones I to III and zone V; (ii) the stacking pattern II<sub>1</sub> is dominant in zone IV; the stacking patterns II<sub>1</sub> and II<sub>2</sub> are both common in zones VI and VII; and (iv) the stacking pattern III is common in zones VII and VIII, as well as the stacking pattern II. In addition, the channel-body density is high in zones VII and VIII, is moderate in zones 4, 6 and 7, and is low in zones I-III and zone V.

### 5. Discussion

River types and channel-body stacking patterns are crucial for understanding relationships between fluvial architecture and A/S changes (Schumm, 1993; Wright and Marriott, 1993; Holbrook et al., 2006); their relationships are discussed in this section.

#### 5.1. Responses of fluvial river type

Under low A/S conditions (stage I), both the outcropping and the subsurface fluvial successions are considered as having been produced by braided fluvial systems (stage I in Table 2; zones 6–8 and

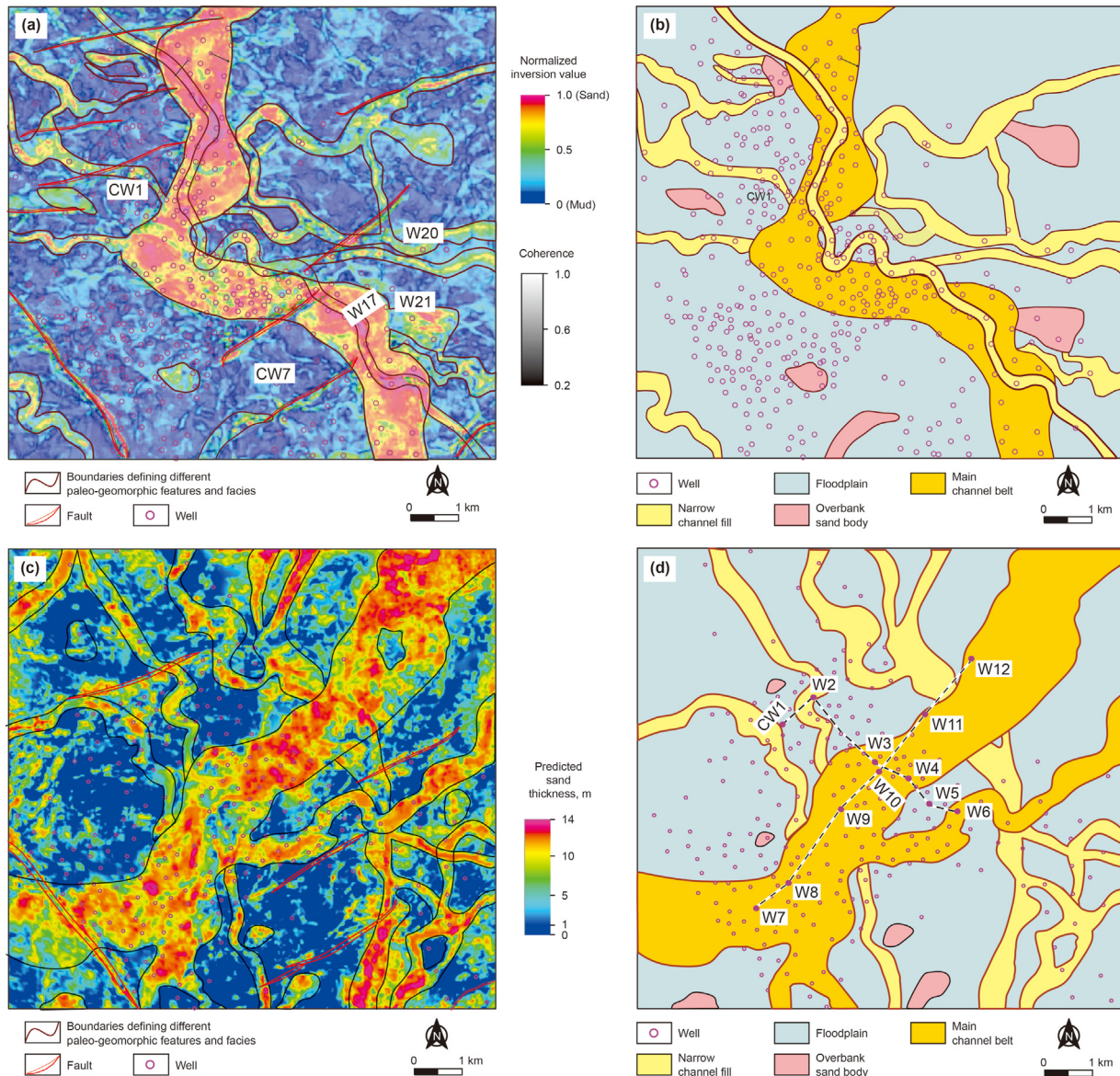


**Fig. 11.** (a) Map of reservoir zone II extracted from the spectral-decomposition genetic inversion cube, which is co-rendered with the coherence attribute. (b) Distribution of fluvial sandbodies in reservoir zone II. (c) Optimized max-peak amplitude attribute of reservoir zone VI, obtained after reducing the interferences of neighboring zones. The fused attribute represents predicted sand thickness. (d) Distribution of fluvial sandbodies in the reservoir zone VI. The well-correlation profile beginning with well “CW1” is corresponding to Fig. 8, and the other well-correlation profile is interpreted below. Parts (a) and (b) were modified after Li et al., 2019b; parts (c) and (d) modified after Li et al., 2021. See Fig. 8 for the well-correlation panel and their well logs.

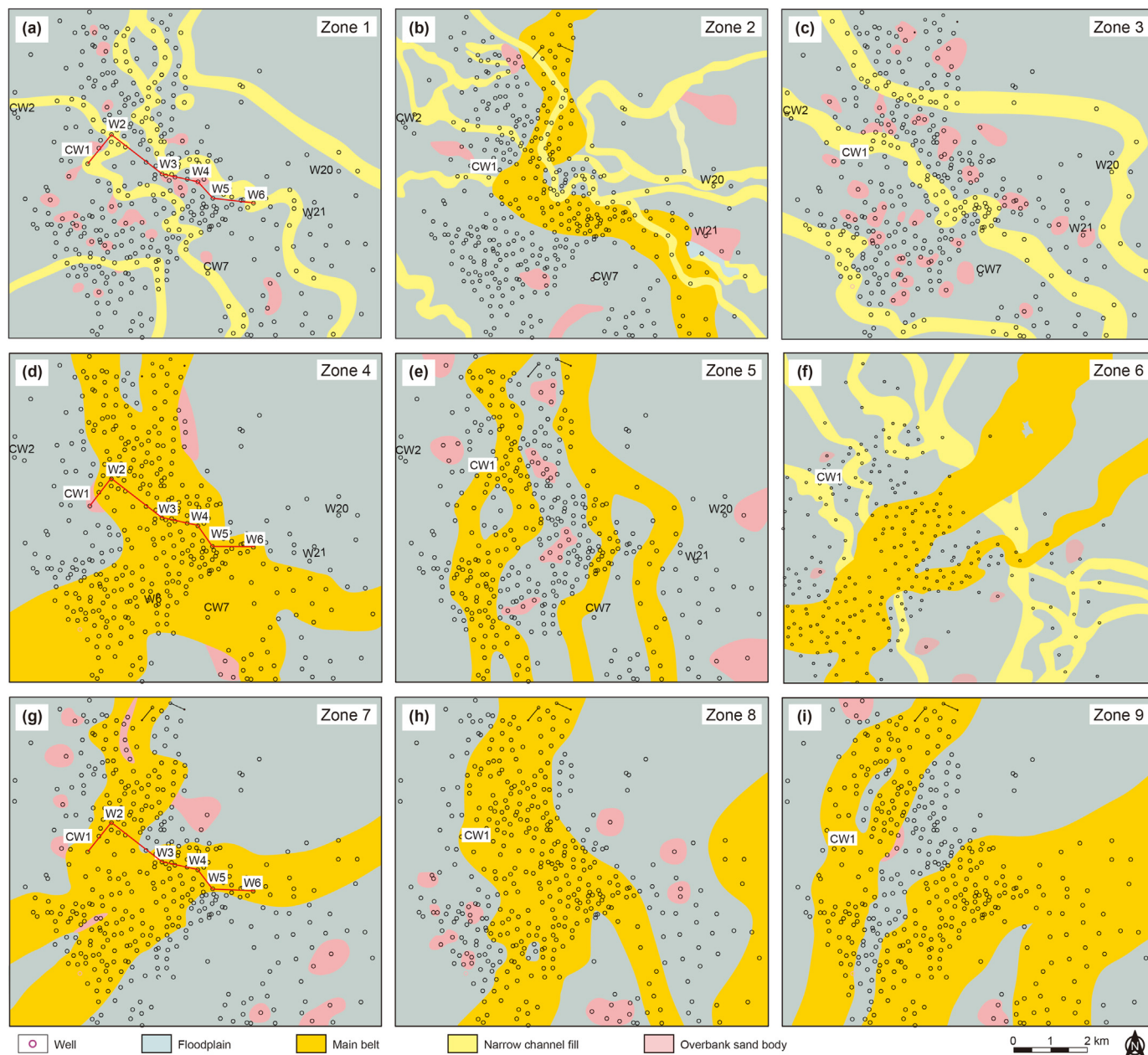


Fig. 12. Maps showing the distribution of fluvial sandbodies in zones I to IX, in the study area. See Fig. 8 for the well-correlation panel and their well logs.

10–11 in Figs. 6 and 7; zone IX in Fig. 10), in which vertical aggradation was predominant in fluvial bars, and braid bars and channel fills were extensively eroded.

When the A/S ratio rises to stage II, the proportion of lateral accretion increases significantly but remains still subordinate relative to vertical aggradation (stage II in Table 2; zones 4–5 in Fig. 7c; zones VII–VIII in Fig. 10). Fluvial successions transitioned to braided-meandering river depositional systems. Both point bars and mid-channel bars may be observed in the same channel belt, although mid-channel bars may be more common. Another distinctive feature is that compound mid-channel bars are commonly separated by a set of thin, fine-grained layers (Fig. 7f). This type of river is also termed a wandering river.

When the A/S ratio increases to stage III, the proportion of lateral accretion increases, becoming more common than vertical aggradation (stage III in Table 2; last-period deposits of zone 5 in Fig. 7c). The fluvial successions are still considered mixed braided-meandering systems, but the deposits produced by meandering rivers account for a higher proportion of deposits.

Eventually, under conditions of high A/S ratio, the subsurface and outcrop successions are considered typical of meandering depositional systems (stage IV in Table 2; Fig. 7b; zones I–III in Figs. 10 and 13). Thus, with further increasing A/S ratio, the braided rivers gradually transition into meandering rivers (Table 2).

**Table 1**

Channel-body stacking patterns, geological models, and their responses of well logs and seismic inversion. Four common stacking patterns and sub-patterns are summarized (see text).

Channel-body stacking pattern	Geological model	Response of well logs and the seismic inversion	Description and interpretation
I. Isolated (one-story)			Isolated channel bodies are encased in floodplain deposits.
Two-story II	II <sub>1</sub> . Stacking in lateral dominantly		Two channel bodies stack laterally, and are connected through a small contact area.
	II <sub>2</sub> . Stacking in vertical dominantly		
III. Multi-story			Channel bodies are densely stacked, forming a compound channel belt or an alluvial-valley fill.

Note: The channel-body density increases from stacking patterns I to III.

5.2. Responses of channel-body stacking pattern to A/S changes

Both channel-body density and stacking patterns show significant variations for different conditions of A/S ratio. When the A/S ratio is low (Stage I in Fig. 14d), channel bodies are stacked in a multi-story pattern and show a very high channel-body density, a situation corresponding to that of zones 7–8 in the outcrop dataset (Fig. 7g and h) and to zone IX in the subsurface dataset (Fig. 13). These stacking channel bodies form a complex, compound channel belt, in which channel erosion surfaces are frequent, and preserved channel bodies are seriously eroded. No or limited floodplain deposits are preserved within the compound channel belt.

Under relatively lower A/S conditions (Stage II in Fig. 14c), both multi-story and two-story stacking patterns are common, a situation corresponding to reservoir zones VII–VIII in the subsurface dataset (Fig. 13) and to zones 9–11 in the outcrop dataset (Figs. 6 and 7). The channel-body density decreases significantly. In the compound channel belt, the frequency of channel erosion surfaces is moderate.

Under conditions of relatively higher A/S ratio (Stage III in Fig. 14b), channel bodies are principally stacked in a two-story pattern, which is in accord with zones IV–VI in the subsurface dataset (Fig. 13) and with zones 4–5 in the outcrop dataset (Fig. 7). The channel-body density is moderate, lower than that in Stages I and II shown in Fig. 14.

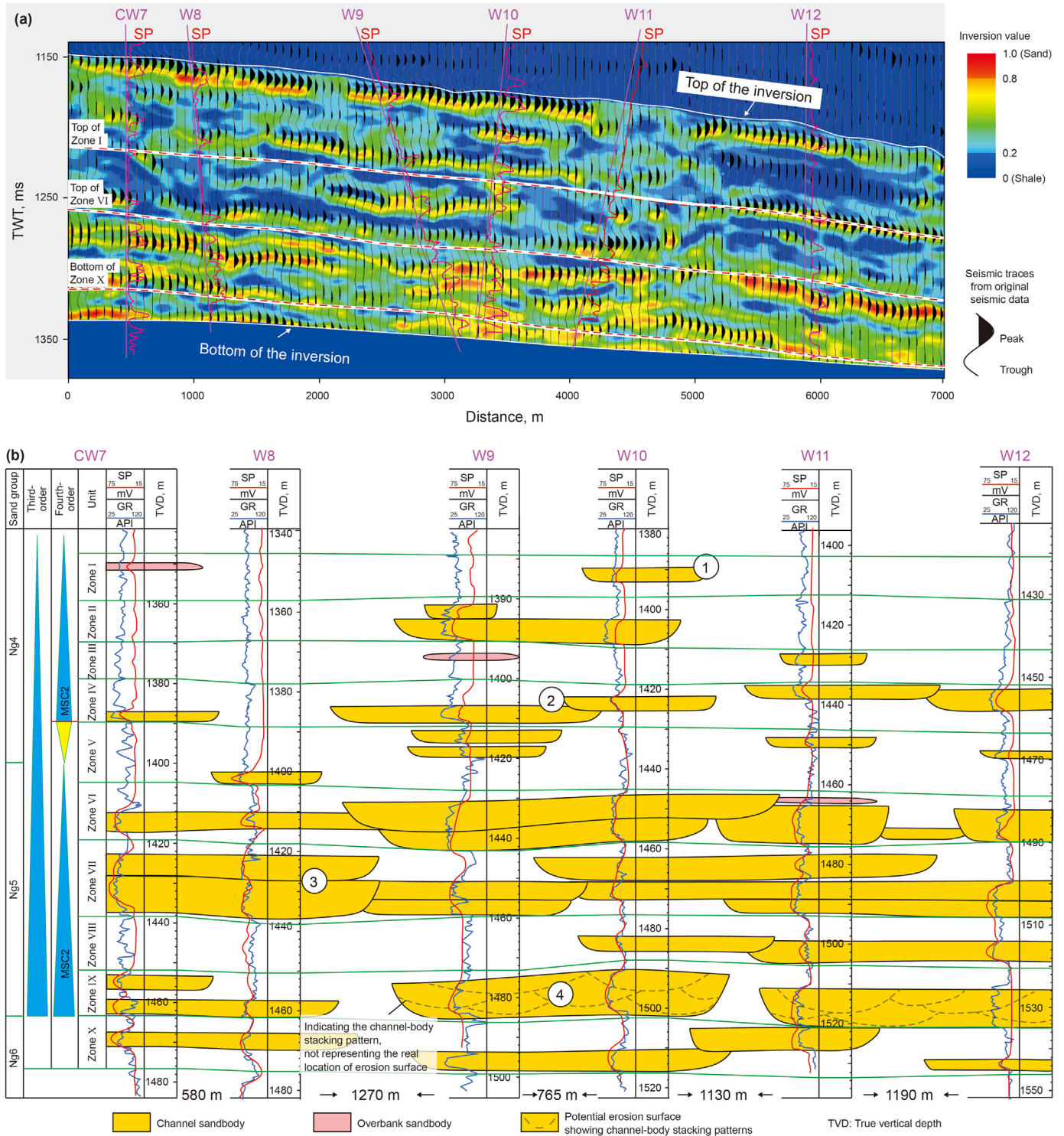
Under high A/S conditions, channel bodies are commonly encased in floodplain strata, showing an isolated stacking pattern, corresponding to zones I–III of the subsurface successions (Fig. 13) and to zones 1–3 of the outcropping successions (Fig. 7). In this

scenario, channel bodies may only be connected locally and through a small contact area.

In brief, along with the rise in A/S ratio, the channel-body density increases, and the stacking patterns vary from multi-story, to two-story and then to isolated (Fig. 14).

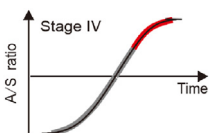
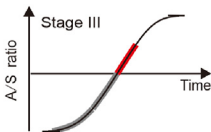
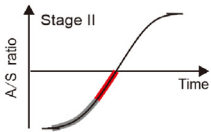
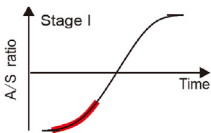
5.3. Applications

Relationships between the A/S ratio and fluvial sedimentary architectures are established in this work, which is a response to the debate topic that whether to apply the sequence stratigraphic models as a fluvial architecture indicator (Miall, 2010; Colombera et al., 2015). These relationships could be applied in researches related to the reconstruction of fluvial sequence stratigraphy and characterization of subsurface fluvial reservoirs. It is a common but challenge work to establish a fluvial sequence framework based on several discontinuous outcrop sections (Miall, 2010), whereas sedimentary architectures can be observed directly on the outcropping fluvial successions. Therefore, the fluvial sequence framework can be established using the established relationships (Catuneanu et al., 2009). On the other hand, fluvial sequence framework can be established based on 3D seismic data and well logs, which can be used to predict changes of fluvial river types and sedimentary architectures. In fact, effects of A/S ratio on fluvial architectures have been used in the characterization of fluvial reservoir (Shanley and McCabe, 1994; Cross, 2000; Miall, 2010), especially in oilfields of China (e.g., Zheng et al., 2001; Deng, 2009; Tan et al., 2020).



**Fig. 13.** (a) A profile from the seismic inversion cube (modified after Li et al., 2019a). (b) Well-correlation panel showing the reservoir zones and distribution of fluvial sandbodies in the Upper Guantao Formation. Areas ① - ④ show four stacking patterns, corresponding to stacking patterns of I, II<sub>1</sub> and III in Table 1, respectively. The location is shown in Fig. 11d. Note: Potential erosion surfaces within channel belt ④ are used to illustrate the channel-body stacking pattern, not to represent the real locations of erosion surfaces (see text).

**Table 2**  
Relationships between the A/S change and formative river types in continental fluvial successions, and their corresponding strata in the subsurface and outcrop datasets.

A/S ratio	Outcropping fluvial successions in the Datong Basin	Subsurface fluvial successions of the Chengdao Oilfield	River type in origin
 <p>Stage IV</p>	Corresponding to zones 1–3	Corresponding to zones I-III	Meandering rivers
 <p>Stage III</p>	Corresponding to the last-period deposits in zones 4	Corresponding to zones IV-VI	Braided-meandering rivers, in which the proportion of lateral aggregations is more than that of lateral aggregations
 <p>Stage II</p>	Corresponding to zones 4–5	Corresponding to zones VII-VIII	Braided-meandering rivers, in which the proportion of vertical aggregations is more than that of lateral aggregations
 <p>Stage I</p>	Corresponding to zones 6–8, and 10-11	Corresponding to zone X	Braided rivers

5.4. Other depositional conditions and limitations

A set of depositional conditions may affect river types and their sedimentary architectures, in which tectonic and climatic conditions are two important controls (Miall, 2010; Li et al., 2015; Yue et al., 2018), as well as A/S conditions. Some researchers argue that tectonic conditions control fluvial rivers though the riverbed gradient to a large degree (Holbrook et al., 2006; Li et al., 2023), and discharge is the link between climate and fluvial formation (Fielding et al., 2018; Hansford and Plink-Björklund, 2020). A rising riverbed gradient results in the fall of river grad, as well as the decrease of fluvial base-level (Holbrook et al., 2006; Li et al., 2022). Climate conditions are commonly divided into humid, subhumid, semiarid or seasonal, and arid climate (Fielding et al., 2018). Arid climates where stream flow is few are not discussed here. Compared to humid and subhumid climates, semiarid climates are associated with a higher flood and a poor vegetation (Fielding et al., 2018), which results in a larger sediment supply and thus lead to a lower A/S. In terms of the humid and subhumid climates, rising discharge would result in increases of both accommodation and sediment supply (Miall, 2010; Li et al., 2023), so changes of A/S are uncertain (Miall, 2010).

Generally, a set of depositional conditions affect fluvial river types, in which A/S ratio is a prominent control. In particular, A/S condition is an integrated factor that can reflect the tectonic, climatic and other conditions to some degree (Cross, 2000; Miall,

2010). Nonetheless, the A/S cannot cover all the depositional conditions, which may affect fluvial architectures.

6. Conclusions

A fluvial outcrop succession has enabled observations at a high resolution of sedimentary features, as well as inference of formative river types. A subsurface fluvial reservoir has been studied in terms of the distribution of channel bodies, which can be mapped clearly integrating a seismic cube with dense well data, which collectively provide a larger, 3D perspective and again enable inference of formative river types. Integration of both datasets has contributed to our understanding of relationships between channel-body stacking patterns, formative river types, and A/S changes.

Along with the increase of A/S, the formative river types of fluvial successions commonly transition from braided planforms to mixed braided-meandering (wandering) planforms and then to meandering ones. In parallel, channel-body stacking patterns change through with the increase in A/S, in the form of multi-story, mixed multi- and two-story, two-story, and isolated patterns. At the same time, the channel-body density decreases along with the transition of channel-body stacking patterns.

Declaration of competing interest

The authors declare that they have no known competing

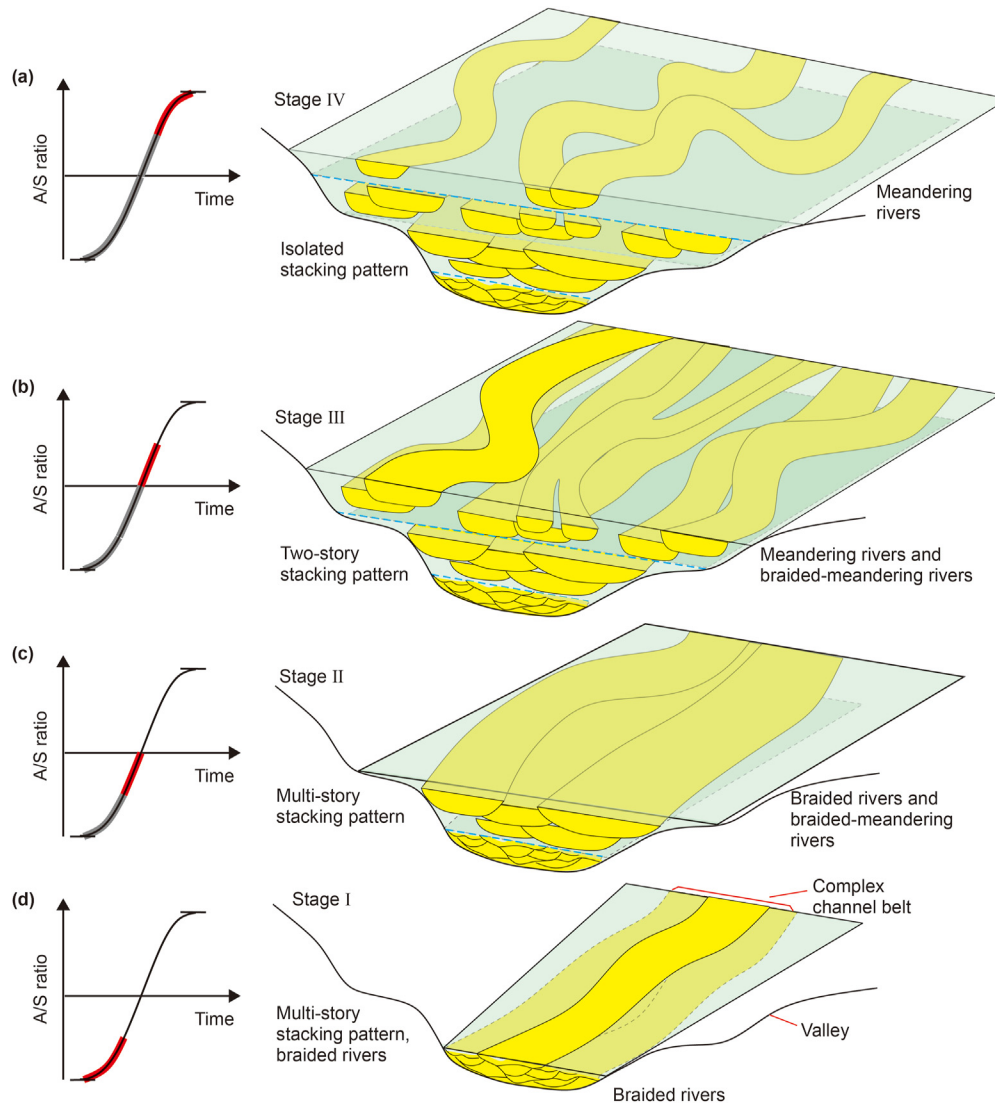


**Fig. 14.** Channel-body density and stacking patterns in different conditions of A/S ratio. (a) In a high A/S condition (stage IV), channel bodies are incised in the floodplain, showing an isolated stacking pattern and a low channel-body density. (b) In a relatively-higher A/S condition (stage III), two-story stacking patterns of channel body are common. (c) In a relatively-lower A/S condition (stage II), both multi- and two-story stacking patterns of channel body are common, with a moderate channel-body density. (d) In a low A/S condition (stage I), multi-story channel-body stacking patterns is the dominant, with a high channel-body density. River types in stages I-IV are corresponding to those in Table 2.

financial interests or personal relationships that could have appeared to influence the work reported in this paper.

## Acknowledgements

This research was financially supported by the National Natural Science Foundation Project of China (No. 42202109, 42272186), the China Postdoctoral Science Foundation (BX20220351, 2022M713458), the Research Institute of Petroleum Exploration and Development, China (2021DJ1101), and the Cooperation Project of the PetroChina Corporation (ZLZX2020-02). Anonymous reviewers are thanked for their constructive comments, which helped improve the paper. Additionally, associate professor Luca Colombera is thanked for his suggestions and language polishing work.

## References

Ainsworth, R.B., McArthur, J.B., Lang, S.C., Vonk, A.J., 2018. Quantitative sequence stratigraphy. *Am. Assoc. Petrol. Geol. Bull.* 102 (10), 1913–1939. <http://doi.org/10.1306/02201817271>.

- Blum, M.D., Törnqvist, T.E., 2000. Fluvial responses to climate and sea-level change: a review and look forward. *Sedimentology* 47 (Suppl. 1), 2–48. <http://doi.org/10.1046/j.1365-3091.2000.00008.x>.
- Catuneanu, O., Abreu, V., Bhattacharya, J.P., Blum, M.D., Dalrymple, R.W., Eriksson, P.G., Fielding, C.R., Fisher, W.L., Galloway, W.E., Giblin, M.R., 2009. Towards the standardization of sequence stratigraphy. *Earth Sci. Rev.* 92 (1–2), 1–33. <http://doi.org/10.1016/j.earscirev.2008.10.003>.
- Colombera, L., Mountney, N.P., McCaffrey, W.D., 2015. A meta-study of relationships between fluvial channel-body stacking pattern and aggradation rate: implications for sequence stratigraphy. *Geology* 43 (4), 283–286. <https://doi.org/10.1130/G36385.1>.
- Colombera, L., Arévalo, O.J., Mountney, N.P., 2017. Fluvial-system response to climate change: the Paleocene-Eocene Tremp group, Pyrenees, Spain. *Global Planet. Change* 157, 1–17. <http://doi.org/10.1016/j.gloplacha.2017.08.011>.
- Colombera, L., Mountney, N.P., 2020. Accommodation and sediment-supply controls on clastic parasequences: a meta-analysis. *Sedimentology* 67, 1667–1709. <https://doi.org/10.1111/sed.12728>.
- Cross, T.A., 2000. Stratigraphic controls on reservoir attributes in continental strata. *Earth Sci. Front.* 7 (4), 322–350.
- Deng, H.W., 2009. Discussion on problems of applying high resolution sequence stratigraphy (in Chinese with English abstract). *J. Palaeogeogr.* 11 (5), 471–480. <https://doi.org/10.7605/gdtxb.2009.05.001>.
- Fanti, F., Catuneanu, O., 2010. Fluvial sequence stratigraphy: the wapiti formation, West-Central Alberta, Canada. *J. Sediment. Res.* 80 (4), 320–338. <https://doi.org/10.1306/02201817271>.



- org/10.2110/jsr.2010.033.
- Fielding, C.R., Alexander, J., Allen, J.P., 2018. The role of discharge variability in the formation and preservation of alluvial sediment bodies. *Sediment. Geol.* 365, 1–20. <https://doi.org/10.1016/j.sedgeo.2017.12.022>.
- Ghinassi, M., Ielpi, A., Aldinucci, M., Fustic, M., 2016. Downstream-migrating fluvial point bars in the rock record. *Sediment. Geol.* 334, 66–96. <https://doi.org/10.1016/j.sedgeo.2016.01.005>.
- Gong, C., Sztanó, O., Steel, R.J., Xian, B.Z., Galloway, W.E., Bada, G., 2019. Critical differences in sediment delivery and partitioning between marine and lacustrine basins: A comparison of marine and lacustrine aggradational to progradational clinotherms pairs. *Bull. Geol. Soc. Am.* 131 (5/6), 766–781. <https://doi.org/10.1130/B32042.1>.
- Hansford, M.R., Plink-Björklund, P., 2020. River discharge variability as the link between climate and fluvial fan formation. *Geology* 48 (10), 952–956. <https://doi.org/10.1130/G47471.1>.
- Holbrook, J., Schumm, S.A., 1999. Geomorphic and sedimentary response of rivers to tectonic deformation: a brief review and critique of a tool for recognizing subtle epirogenic deformation in modern and ancient settings. *Tectonophysics* 305, 287–306. [https://doi.org/10.1016/S0040-1951\(99\)00011-6](https://doi.org/10.1016/S0040-1951(99)00011-6).
- Holbrook, J., Scott, R.W., Oboh-Ikuenobe, F.E., 2006. Base-level buffers and buttresses: a model for upstream versus downstream control on fluvial geometry and architecture within sequences. *J. Sediment. Res.* 76, 162–174. <https://doi.org/10.2110/jsr.2005.10>.
- Howard, A.D., Dietrich, W.E., Seidl, M.A., 1994. Modeling fluvial erosion on regional to continental scale. *J. Geophys. Res.* 99 (B7), 13971–13986. <https://doi.org/10.1029/94JB00744>.
- Jervey, M.T., 1988. Quantitative geological modeling of siliciclastic rock sequences and their seismic expression. In: Wilgus, C.K., Hastings, B.S., Posamentier, H., et al. (Eds.), *Sea-Level Change: an Integrated Approach*. SEPM Special Publication No.42, Mira Digital Publishing, Tulsa, pp. 47–69.
- Knighton, D., 1988. *Fluvial Forms and Processes*, first ed. Hodder Arnold, London <https://doi.org/10.4324/9780203784662>.
- Li, S.L., Yu, X.H., Chen, B.T., Li, S.L., 2015. Quantitative characterization of architecture elements and their response to base-level change in a sandy braided fluvial system at a mountain front. *J. Sediment. Res.* 85 (10), 1258–1274. <https://doi.org/10.2110/jsr.2015.82>.
- Li, W., Yue, D.L., Colombera, L., et al., 2021. Quantitative prediction of fluvial sandbodies by combining seismic attributes of neighboring zones. *J. Pet. Sci. Eng.* 196, 107749. <https://doi.org/10.1016/j.petrol.2020.107749>.
- Li, W., Yue, D.L., Colombera, L., et al., 2020a. A novel method for estimating sandbody compaction in fluvial successions. *Sediment. Geol.* 404, 105675. <https://doi.org/10.1016/j.sedgeo.2020.105675>.
- Li, W., Yue, D.L., Wang, W.F., et al., 2019a. Fusing multiple frequency-decomposed seismic attributes with machine learning for thickness prediction and sedimentary facies interpretation in fluvial reservoirs. *J. Pet. Sci. Eng.* 177, 1087–1102. <https://doi.org/10.1016/j.petrol.2019.03.017>.
- Li, W., Yue, D.L., Wu, S.H., et al., 2020b. Thickness prediction for high-resolution stratigraphic interpretation by fusing seismic attributes of target and neighboring zones with an SVR algorithm. *Mar. Petrol. Geol.* 113, 104153. <https://doi.org/10.1016/j.marpetgeo.2019.104153>.
- Li, W., Yue, D.L., Wu, S.H., et al., 2019b. Characterizing meander belts and point bars in fluvial reservoirs by combining spectral decomposition and genetic inversion. *Mar. Petrol. Geol.* 105, 168–184. <https://doi.org/10.1016/j.marpetgeo.2019.04.015>.
- Li, W., Yue, D.L., Li, J., et al., 2022. Variable architecture models of Fluvial reservoir controlled by base-level cycle: a case study of Jurassic outcrop in Datong basin (in Chinese with English abstract). *Earth Sci.* 47 (11), 3929–3943. <https://doi.org/10.3799/dqkx.2022.221>.
- Li, W., Colombera, L., Yue, D.L., Mountney, N.P., 2023. Controls on the morphology of braided rivers and braid bars: an empirical characterization of numerical models. *Sedimentology* 70 (1), 259–279. <https://doi.org/10.1111/sed.13040>.
- Mackin, J.H., 1948. Concept of the graded river. *Geol. Soc. Am. Bull.* 59, 463–512. [https://doi.org/10.1130/0016-7606\(1948\)59\[463:COTGR\]2.0.CO;2](https://doi.org/10.1130/0016-7606(1948)59[463:COTGR]2.0.CO;2).
- Martinius, A.W., Effenbein, C., Keogh, K.J., 2014. Applying accommodation versus sediment supply ratio concepts to stratigraphic analysis and zonation of a fluvial reservoir. In: Martinius, A.W., Ravnäs, R., Howell, J.A. (Eds.), et al., *Depositional Systems to Sedimentary Successions on the Norwegian Continental Margin*, first ed. John Wiley & Sons, Ltd. IAS Special Publication No.46, pp. 101–125 <https://doi.org/10.1002/9781118920435.ch4>.
- Melo, A.H., Magalhães, A.J.C., Menegazzo, M.C., et al., 2021. High-resolution sequence stratigraphy applied for the improvement of hydrocarbon production and reserves: a case study in Cretaceous fluvial deposits of the Potiguar basin, northeast Brazil. *Mar. Petrol. Geol.* 130, 105124. <https://doi.org/10.1016/j.marpetgeo.2021.105124>.
- Merritts, D.J., Vincent, K.R., Wohl, E.E., 1994. Long river profiles, tectonism, and eustasy: a guide to interpreting fluvial terraces. *J. Geophys. Res.* 99 (B7), 14031–14050. <https://doi.org/10.1029/94JB00857>.
- Miall, A.D., 1991. Stratigraphic sequences and their chronostratigraphic correlation. *J. Sediment. Petrol.* 61, 497–505. <https://doi.org/10.1306/D4267744-2B26-11D7-8648000102C1865D>.
- Miall, A.D., 2010. *The Geology of Stratigraphic Sequences*, second ed. Springer-Verlag, Heidelberg, pp. 47–72 <https://doi.org/10.1007/978-3-642-05027-5>.
- Mueller, E.R., Pitlick, J., 2014. Sediment supply and channel morphology in mountain river systems: 2. Single thread to braided transitions. *J. Geophys. Res. Earth Surf.* 119, 1516–1541. <https://doi.org/10.1002/2013JF003045>.
- Posamentier, H.W., Jervey, M.T., Vail, P.R., 1988. Eustatic controls on clastic deposition I—conceptual Framework. In: Wilgus, C.K., Hastings, B.S., Posamentier, H. (Eds.), et al., *Sea-Level Change: an Integrated Approach*. SEPM Special Publication No.42, Mira Digital Publishing, Tulsa, pp. 109–124. <https://doi.org/10.2110/pec.88.01.0109>.
- Posamentier, H.W., Vail, P.R., 1988. Eustatic controls on clastic deposition II—sequence and systems tract models. In: Wilgus, C.K., Hastings, B.S., Posamentier, H. (Eds.), et al., *Sea-Level Change: an Integrated Approach*. SEPM Special Publication No.42, Mira Digital Publishing, Tulsa, pp. 125–154. <https://doi.org/10.2110/pec.88.01.0109>.
- Ren, X.X., Hou, J.G., Liu, Y.M., Chen, D.P., Zhang, X.Y., 2018. Architectural characterization and a distribution model of lithology near the boundary surfaces of different orders in a sandy braided river: a case study from the Jurassic sandy braided-river outcrops in the Datong Basin, Shanxi Province (In Chinese with English abstract). *Pet. Sci. Bull.* 3 (3), 245–261.
- Rider, M.H., 1990. Gamma-ray log shape used as a facies indicator: critical analysis of an oversimplified methodology. *Geol. Soc. Spec. Publ.* 48, 27–37. <https://doi.org/10.1144/GSL.SP.1990.048.01.04>.
- Rook, L., Ghinassi, M., Libsekal, Y., et al., 2010. Stratigraphic context and taxonomic assessment of the large cercopithecoid (Primates, Mammalia) from the late Early Pleistocene palaeoanthropological site of Buia (Eritrea). *J. Hum. Evol.* 59 (6), 692–697. <https://doi.org/10.1016/j.jhevol.2010.07.018>.
- Schumm, S.A., 1993. River response to baselevel change: implications for sequence stratigraphy. *J. Geol.* 101 (2), 279–294. <https://doi.org/10.1086/648221>.
- Schumm, S.A., 2005. *River Variability and Complexity*, first ed. Cambridge University Press, New York, p. 220 <https://doi.org/10.1017/CBO9781139165440>.
- Shanley, K.W., McCabe, P.J., 1994. Perspectives on the sequence stratigraphy of continental strata. *Am. Assoc. Petrol. Geol. Bull.* 78 (4), 544–568. <https://doi.org/10.1306/BDF9258-1718-11D7-8645000102C1865D>.
- Tan, M.X., Zhu, X.M., Zhang, Z.L., Liu, Q.H., Shi, W.L., 2020. Fluvial sequence pattern and its response of geomorphology in depression phase of rift basin: a case study of the Lower Member of Neogene Minghuazhen Formation in Shaleitian Uplift area, Bohai Bay Basin (in Chinese with English abstract). *Journal of Palaeogeography* 22 (3), 428–439. <https://doi.org/10.7605/gdxb.2020.03.029>.
- Tebbens, L.A., Veldkamp, A., Van Dijke, J.J., School, J.M., 2000. Modeling longitudinal profile development in response to Late Quaternary tectonics, climate and sea-level changes: the River Meuse. *Global Planet. Change* 27, 165–186. [https://doi.org/10.1016/S0921-8181\(01\)00065-0](https://doi.org/10.1016/S0921-8181(01)00065-0).
- Trampush, S.M., Huzurbazar, S., McElroy, B., 2014. Empirical assessment of theory for bankfull characteristics of alluvial channels. *Water Resour. Res.* 50, 9211–9220. <https://doi.org/10.1002/2014WR016527>.
- Wang, S., 2001. Fluvial depositional systems and river pattern evolution of middle Jurassic series, Datong basin (in Chinese with English abstract). *Acta Sedimentol. Sin.* 19 (4), 501–505. <https://doi.org/10.14027/j.cnki.cjxh.2001.04.005>.
- Wescott, W.A., 1993. Geomorphic thresholds and complex response of fluvial systems—some implications for sequence stratigraphy. *Am. Assoc. Petrol. Geol. Bull.* 77 (7), 1208–1218. <https://doi.org/10.1306/BDF8E3E-1718-11D7-8645000102C1865D>.
- Wright, V.P., Marriott, S.B., 1993. The sequence stratigraphy of fluvial depositional systems: the role of floodplain sediment storage. *Sediment. Geol.* 86, 203–210. [https://doi.org/10.1016/0037-0738\(93\)90022-W](https://doi.org/10.1016/0037-0738(93)90022-W).
- Yan, N., Colombera, L., Mountney, N.P., 2020. Three-dimensional forward stratigraphic modelling of the sedimentary architecture of meandering-river successions in evolving half-graben rift basins. *Basin Res* 32 (1), 68–90. <https://doi.org/10.1111/bre.12367>.
- Yao, Z.Q., Yu, X.H., Shan, X., et al., 2018. Braided-meandering system evolution in the rock record: implications for climate control on the Middle–Upper Jurassic in the southern Junggar Basin, north-west China. *Geol. J.* 53 (6), 2710–2731. <https://doi.org/10.1002/gj.3105>.
- Yu, X.H., Ma, X.X., Qing, H.R., 2002. *Sedimentology and reservoir characteristics of a Middle Jurassic fluvial system, Datong Basin, northern China*. *Bull. Can. Pet. Geol.* 50 (1), 105–117.
- Yue, D.L., Li, W., Wang, J., Wang, W.R., Li, J., 2018. Prediction of meandering belt and point-bar recognition based on spectral-decomposed and fused seismic attributes: a case study of the Guantao Formation, Chengdao Oilfield, Bohai Bay Basin (in Chinese with English abstract). *J. Palaeogeogr.* 20 (6), 941–950. <https://doi.org/10.7605/gdxb.2018.06.068>.
- Zheng, H.R., Lin, H.X., Wang, Y.S., 2000. Practice and knowledge of exploration on Chengdao oil field (in Chinese with English abstract). *Petrol. Explor. Dev.* 12 (6), 1–9.
- Zheng, R.C., Peng, J., Wu, C., 2001. Grade division of base-level cycles of terrigenous basin and its implications (in Chinese with English abstract). *Acta Sedimentol. Sin.* 19 (2), 249–255. <https://doi.org/10.14027/j.cnki.cjxh.2001.02.014>.